In situ transmission electron microscopy of individual carbon nanotetrahedron/ribbon structures in bending

Hideo Kohno[1,a)] and Yusuke Masuda[2]
[1]*School of Environmental Science and Engineering, Kochi University of Technology, Kami, Kochi 782-8502, Japan*
[2]*Graduate School of Science, Osaka University, Toyonaka, Osaka 560-0043, Japan*

(Received 25 January 2015; accepted 30 April 2015; published online 12 May 2015)

When the direction of flattening of a carbon nanotube changes during growth mediated by a metal nanoparticle, a carbon nanotetrahedron is formed in the middle of the carbon nanoribbon. We report the bending properties of the carbon nanotetrahedron/nanoribbon structure using a micromanipulator system in a transmission electron microscope. In many cases, bending occurs at an edge of the carbon nanotetrahedron. No significant change is observed in the tetrahedron's shape during bending, and the bending is reversible and repeatable. Our results show that the carbon nanotetrahedron/nanoribbon structure has good durability against mechanical bending. © *2015 AIP Publishing LLC*. [http://dx.doi.org/10.1063/1.4921008]

Durability against mechanical bending is important even for nanomaterials when they are used in flexible devices. Carbon nanotubes (CNTs)[1] are good candidate materials for flexible devices because of their excellent mechanical properties in addition to their unique electrical and thermal properties. Mechanical properties of CNTs have been investigated by many groups.[2–10] For example, Falvo *et al.* examined the behavior of multi-walled carbon nanotubes (MWCNTs) under large strain and found that MWCNTs could be bent repeatedly through large angles without undergoing catastrophic failure.[5]

In our previous paper, we reported that a change in the direction of flattening of a carbon nanotube, grown from an Fe catalyst particle by chemical vapor deposition (CVD), resulted in the formation of a carbon nanotetrahedron in the middle of a carbon nanoribbon.[11] We expect that the carbon nanotetrahedron/nanoribbon structure inherits the excellent properties of CNTs and carbon nanoribbons. Furthermore, it might be possible to obtain additional unique properties owing to the presence of the carbon nanotetrahedra or to find ways of utilizing the structure's characteristics. An example would be to use the structure for three-dimensional wiring, exploiting its shape having two directions of flattening. In order to examine whether our carbon nanotetrahedron/nanoribbon structures can be used for this purpose, we have examined their durability against Joule heating in a transmission electron microscope, and revealed that the nanotetrahedra were as stable as CNTs.[12] When using the carbon nanotetrahedron/nanoribbon structure in flexible devices, it is also important to understand its durability against mechanical strain. In this paper, we focus on the mechanical behavior of the carbon nanotetrahedron/nanoribbon structure under bending. Its structure during bending is observed *in situ* in a TEM.

In our simplified CVD growth of carbon nanotetrahedron/nanoribbon structures, a 20-nm-thick layer of Fe was deposited on a Si (100) substrate, whose surface was roughened using SiC powder to obtain a fresh surface. Then, the sample was sealed in an evacuated silica tube (inner diameter = 6 mm; length ≈ 20 cm) with 0.8 mg of hexadecanoic acid [$C_{15}H_{31}C(=O)OH$] as a carbon source. The sample was heated at 1000 °C for 30 min, then cooled to room temperature after the growth. The grown carbon nanostructures were mounted on a Au wire by scratching the Au wire on the substrate on which the carbon nanostructures were grown for in situ TEM observation of bending. The Au wire was mounted on a TEM sample holder equipped with a piezo-driven micromanipulator. An electrochemically sharpened W needle was used as a mobile probe. Charge coupled device (CCD) camera images were recorded at a frame rate of about 2.6 fps with a resolution of 512 × 512 pixels during *in situ* observations of bending. For simple TEM observations, the carbon nanotetrahedron/nanoribbon structures were mounted on a carbon microgrid. For scanning electron microscopy (SEM) observations, the Si substrate was used directly.

Typical SEM and TEM micrographs, and electron micro-diffraction patterns, for a carbon nanotetrahedron/nanoribbon structure are shown in Fig. 1 with schematic illustrations. The electron diffraction patterns and the high-resolution TEM image clearly reveal the structure's graphitic nature, and the series of TEM images viewed along different directions show its three-dimensional form. The inner wall of a nanoribbon does not exhibit clear contrast in TEM images since the curvature of the innermost wall at the edge is very large when a CNT flattens, while the inner wall of a CNT shows up very clearly in a TEM image. This enables us to distinguish a nanoribbon from a nanotube in plan-view TEM imaging. MWCNTs with a wall number of around 10–20 flattened to form nanotetrahedron/nanoribbon structures. The width of nanoribbons was tens of nanometers, which defined the size of the carbon nanotetrahedra. Each nanoribbon had nearly the same width, owing to the high crystallinity of the original MWCNT. The edge of the nanotetrahedron, which was perpendicular to the viewing direction in the TEM image, was unclear, while the planes parallel to the viewing direction appeared with good contrast, in agreement with the

[a)]kohno.hideo@kochi-tech.ac.jp; http://www.scsci.kochi-tech.ac.jp/kohno/

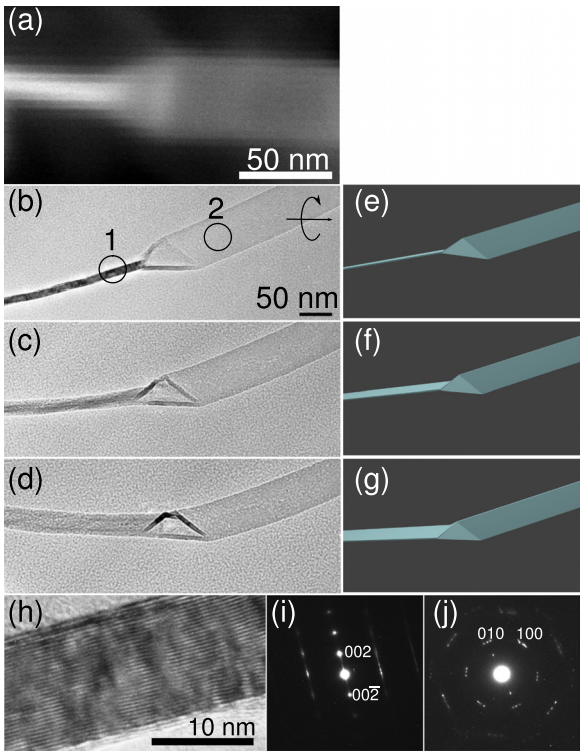

FIG. 1. (a) SEM image of a carbon nanotetrahedron/ribbon structure. (b)–(d) TEM images of a carbon nanotetrahedron/ribbon viewed along different directions: from (b) to (c) 15.8° and from (c) to (d) 9.8°. (e)–(g) Three-dimensional (3D) model of the structure viewed along various directions. (h) High-resolution TEM image taken around position #1 in (b), resolving the graphite (002) lattice fringes. (i) and (j) Electron diffraction patterns taken from positions #1 and #2, respectively. The diffraction patterns in (i) and (j) were taken with, respectively, electron beams parallel and normal to the graphite (002) planes.

geometry of the nanotetrahedron. In the SEM image, the edge of a nanotetrahedron perpendicular to the viewing direction was more visible than that in the TEM image, presumably owing to the edge effect, since the angle between the electron beam and the nanoribbon surface and that between the electron beam and a plane in the nanotetrahedron connected to the nanoribbon were different.

An example of the bending behavior of a carbon nanotetrahedron/ribbon structure is shown in Fig. 2 and its multimedia view. The nanoribbon was twisted at the position indicated by the arrowhead. Although the twist looks similar to the nanotetrahedron, it can be distinguished from the nanotetrahedron (indicated by the arrow). The contact between the nanoribbon and the mobile probe was due to the van der Waals force, and we did not fix the contact with contamination-deposition by a focused electron beam. In this example, the microprobe was moved from right to left to push and bend the nanoribbon/tetrahedron structure, and then retracted from left to right. During the pushing movement, the nanoribbon/tetrahedron began to bend at the left edge of the nanotetrahedron connected to the nanoribbon [Fig. 2(b)]. Eventually, the bending angle became larger than a right angle [Fig. 2(c)]. The nanoribbon on the left side of the nanotetrahedron described a convex arc before being bent, which became concave upon bending. The bend in the left nanoribbon was not as sharp as that at the junction of the nanoribbon and nanotetrahedron. When the microprobe was

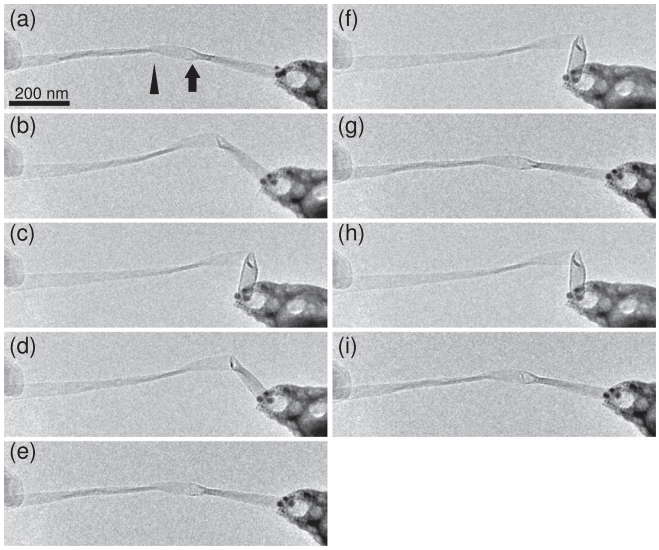

FIG. 2. Series of TEM images of the bending of a carbon nanotetrahedron/nanoribbon structure. A mobile W probe is attached to the right end of the ribbon. The arrow indicates a nanotetrahedron. The nanoribbon is twisted at the position indicated by the arrowhead. (a)–(e) First cycle, (f) and (g) second cycle, and (h) and (i) third cycle. Also see the movie. (Multimedia view) [URL: http://dx.doi.org/10.1063/1.4921008.1]

retracted to its original position, the nanoribbon/nanotetrahedron structure returned to its original form, and no marked change was observed in the shape or position of the nanotetrahedron. The nanotetrahedron/ribbon structure was subjected to three cycles of bending. We did not observe any marked difference in the behavior of the structure between the cycles. The bending was reversible and repeatable.

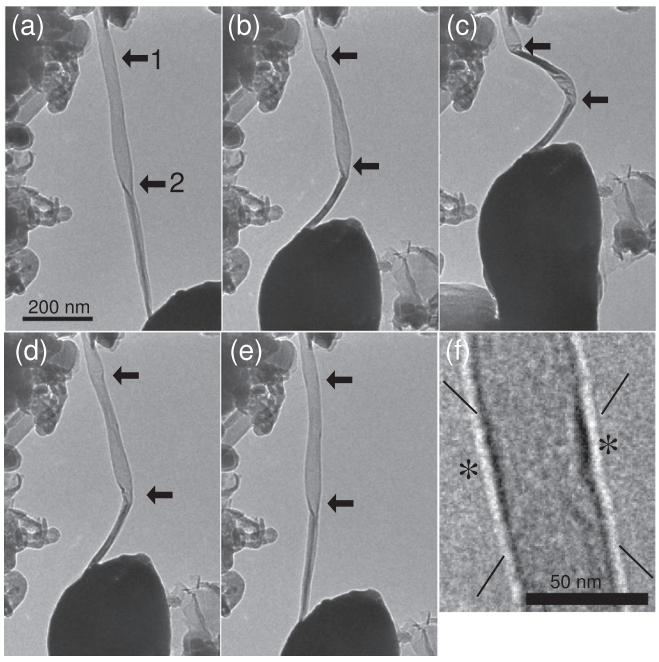

FIG. 3. (a)–(e) Series of TEM images of the bending of a carbon nanoribbon with two carbon nanotetrahedra (indicated by arrows). (f) Enlarged TEM image of the nanotetrahedron #1. The lines indicate the approximate positions of two of the six edges of the nanotetrahedron. The edges of the nanoribbon are clearer around the positions indicated by the asterisks, owing to the presence of the nanotetrahedron. The nanotetrahedron can be recognized clearly in (c). Also see the movie. (Multimedia view) [URL: http://dx.doi.org/10.1063/1.4921008.2]

The second example shows the bending behavior of a nanoribbon with two nanotetrahedra [Fig. 3 and its multimedia view]. The number of graphite layers was measured to be 11×2 from a high-resolution TEM image. The nanotetrahedron #1 was not as clear as the nanotetrahedron #2 in (a) and (e); however, an enlarged image (f) showed two pieces of evidence for the existence of the nanotetrahedron #1 before bending: two faint lines of edges of the nanotetrahedron [indicated by the lines in Fig. 3] and the clear contrast of the edges of the nanoribbon around the position indicated by the asterisks. When the microprobe was pushed toward the nanoribbon/nanotetrahedra, the first sharp bending occurred at the bottom edge of the nanotetrahedron #2, where the nanotetrahedron was connected with the nanoribbon [Fig. 3(b)]. Further pushing resulted in an additional sharp bending at the bottom edge of the nanotetrahedron #1 [Fig. 3(c)]. When the microprobe was retracted, the nanoribbon/nanotetrahedra structure returned to its original form [Figs. 3(d) and 3(e)]. Again, we observed no marked change in the shape or position of the nanotetrahedra, and the nanoribbon remained flattened during and after the bending.

We estimate the force required to bend individual nanoribbon/nanotetrahedron structure at a junction, using the TEM images in Figs. 2 and 3. Since the viewing direction was not necessarily ideal for this type of analysis, we note that the following calculations give only rough estimations. In our calculations, we compared the projected lengths of the nanoribbon before and after the bending to obtain three-dimensional configuration of the nanostructure. The force F normal to the tip of the cantilever can be calculated using the following formula:

$$F = \frac{dEbh^3}{4l^3},$$

where d—tip displacement normal to the unbent cantilever, E—Young's modulus, b—cantilever width, h—thickness, and l—length. We assumed the Young's modulus of the carbon nanoribbon to be 1 TPa.[13] Using this equation, the Young's modulus value, and other values measured from the TEM images, we obtained 3.5 nN, 3.5 nN, and 0.52 nN as the force for the bending #2 in Fig. 3(b), #1 in Fig. 3(c), and in Fig. 2, respectively. Thus, we estimate that a force of 10^{-1} – 10^{0} nN is required to make a sharp bend at a nanoribbon/nanotetrahedron junction. We note that this is smaller than the compressive force reported for the buckling and kinking of a single MWCNT[6] (10^{0} – 10^{1} nN) presumably owing to the difference in shape, namely, moment of inertia of area.

The value of moment of inertia of area of the nanoribbon whose plane is normal to the bending direction is much smaller than that of the opposite nanoribbon whose plane is parallel to the bending direction, and the connecting nanotetrahedron. Thus, the bending moment concentrates on the junction of the perpendicular nanoribbon and the nanotetrahedron. It seems that this caused the sharp bending at the nanotetrahedron/nanoribbon junction.

We have monitored the bending of carbon nanotetrahedron/nanoribbon structures by means of *in situ* TEM using a microprobe system. Our observations showed that bending occurred at the junction of the nanotetrahedron and nanoribbon, i.e., at the edge of the nanotetrahedron. The bending was repeatable and reversible, and the nanotetrahedron showed excellent durability against bending: The nanotetrahedron did not change its position in the nanoribbon, nor did it break. Our results suggest that the present nanotetrahedron/nanoribbon structures can potentially find application in flexible devices, since they can retain their structure during bending. Since it is possible to form a sharp bend at the nanotetrahedron/nanoribbon junction, we expect that these structures can also be used to form three-dimensional wiring: The junction would serve to change the wiring direction.

This work was supported in part by the Adaptable and Seamless Technology Transfer Program through Target-driven R&D, Japan Science and Technology Agency. The authors thank T. Hasegawa, S. Ichikawa, S. Takeda, and H. Yoshida for support. H.K. is grateful to Y. Ohno and I. Yonenaga for the support through the inter-university cooperative research program of the Institute for Materials Research, Tohoku University.

[1]S. Iijima, Nature **354**, 56 (1991).
[2]S. Iijima, C. Brabec, A. Maiti, and J. Bernholc, J. Chem. Phys. **104**, 2089 (1996).
[3]C. Q. Ru, Phys. Rev. B **62**, 9973 (2000).
[4]O. Lourie M.-F. Yu, M. J. Dyer, K. Moloni, T. F. Kelly, and R. S. Ruoff, Science **287**, 637 (2000).
[5]M. R. Favlo, G. J. Clary, R. M. Taylor II, V. Chi, F. P. Brooks, Jr., S. Washburn, and R. Superfine, Nature **389**, 582 (1997).
[6]K. Jensen, W. Mickelson, A. Kis, and A. Zettl, Phys Rev. B **76**, 195436 (2007).
[7]X. Huang, H. Yuan, K. J. Hsia, and S. Zhang, Nano Res. **3**, 32 (2010).
[8]A. Ranjbartoreh and G. Wang, Nanoscale Res. Lett. **6**, 28 (2011).
[9]X. Duan, C. Tang, J. Zhang, W. Guo, and Z. Liu, Nano Lett. **7**, 143 (2007).
[10]J. Zhao, M. R. He, S. Dai, J. Q. Huang, F. Wei, and J. Zhu, Carbon **49**, 206 (2011).
[11]H. Kohno, T. Komine, T. Hasegawa, H. Niioka, and S. Ichikawa, Nanoscale **5**, 570 (2013).
[12]Y. Masuda, H. Yoshida, S. Takeda, and H. Kohno, Appl. Phys. Lett. **105**, 083107 (2014).
[13]M. Meo and M. Rossi, Compos. Sci. Technol. **66**, 1597 (2006).